Original Paper

Cellular Physiology and Biochemistry

Cell Physiol Biochem 2008;22:137-146

Accepted: June 04, 2008

Chondroitin Sulfates Act as Extracellular Gating Modifiers on Voltage-Dependent Ion Channels

Davide Vigetti[1,*], Olga Andrini[1,2,*], Moira Clerici[1], Daniela Negrini[1], Alberto Passi[1] and Andrea Moriondo[1]

[1]Università dell'Insubria, Dipartimento di Scienze Biomediche, Sperimentali e Cliniche, Varese, [2]present address: University of Zurich, Institute of Physiology, Zürich, *Both authors contributed equally to this work.

Key Words
Chondroitin sulfate • Extracellular matrix • Photoreceptor • Ion channels • Xenopus • Calcium

Abstract
Background/Aims. Chondroitin sulfates are glycosaminoglycans bound to core proteins of proteoglycans in the extracellular matrix and perineuronal nets surrounding many types of neurones. Chondroitin 4- and chondroitin 6- sulfate can bind calcium ions with different affinities, depending on their sulfation position. Extracellular calcium plays a key role in determining the transmembrane potential sensed by voltage-operated ion channels (VOCs) by means of the "surface screening effect" theory (Gouy-Chapman-Stern theory). We wanted to test whether chondroitin sulfates at physiological concentration can effectively modulate the gating properties of VOCs. Methods. We recorded in patch-clamp experiments the shift of *h* and voltage-dependent calcium currents activation curves of *Xenopus laevis* photoreceptors perfused with chondroitin sulfate solutions in physiological extracellular calcium concentration. Results. We found that chondroitin 4- and 6- sulfate, with different capabilities, can shift the activation curve of *h* and voltage-dependent calcium channels, compatibly with the surface screening effect theory. Conclusion. We conclude that chondroitin sulfates can alter VOCs gating by modulating the calcium concentration in the extracellular microenvironment. This phenomenon may explain why alterations in the chondroitin sulfation and abundance in the extracellular matrix are found along with altered neuronal function in pathological conditions.

Introduction

Cells are surrounded by a complex extra-cellular matrix (ECM) and receive nutrients and signals from it. Among the different types of molecules that compose ECM, glycosaminoglycans (GAGs) have different chemical, physical, mechanical and biological properties [1, 2]. Chondroitin sulfates (CSs) are a heterogenic group of GAGs bound to a core protein of proteoglycans (PG). CSs consist of repeating disaccharide units formed by D-glucuronic acid β (1-3)D-N-acetyl galactosamine β (1-4). They can be sulfated at positions 4 (CS4) or 6 (CS6) of N-acetyl galactosamine, or in position 2 of the uronic acid. Sulfation is critical to modulate the PGs interaction

KARGER
Fax +41 61 306 12 34
E-Mail karger@karger.ch
www.karger.com

1015-8987/08/0224-0137$24.50/0

Accessible online at:
www.karger.com/cpb

Dr. Andrea Moriondo, Ph.D.
Università dell'Insubria
DSBSC, Via J.H. Dunant, 5 I-21100 Varese (Italy)
Tel. +39 0332 397170, Fax +39 0332 397119
E-Mail: andrea.moriondo@uninsubria.it

with other molecules, like growth factors and chemokines [2].

Cations can be chelated by negatively charged sulfate and carboxylic residues and GAG sulfation pattern plays a fundamental role in determining whether the polysaccharide chains have the capability to bind calcium ions. In this respect, it is known that CS4 has a higher calcium chelating capability than CS6 and hyaluronan, the only unsulfated GAG [3]. While calcium binding to other GAGs like heparin has a critical role in blood coagulation, the physiological functions of the metal chelating capabilities of other GAGs are not clear yet.

In response to various physiopathological stimuli, such as inflammation, a remodelling of ECM occurs, determining a change in GAGs composition and sulfation pattern [4, 5]. This remodelling is due to the action of different enzymes such proteases, glycosidases and sulfatases that are known to be activated in several pathological conditions. These enzymes can dramatically modify the chelating capability of GAGs, altering the free calcium concentration at the outer cell membrane surface.

Extracellular free calcium is essential in cellular processes such as neurotransmitter release and muscle contraction. Moreover, the extracellular free calcium concentration also modulates the transmembrane potential by a phenomenon known as "surface potential theory" (Gouy-Chapman-Stern theory, [6]). In fact, membrane phospholipids carry a net negative charge (due to their polar heads), that can be subject to varying degrees of "screening" by means of positively charged divalent cations. This phenomenon can lead to a different transmembrane voltage drop with respect to the average voltage difference across the two compartments. Given that the voltage sensor moiety of ion channels is embedded in the thickness of the cell membrane, it responds to the actual voltage drop across the membrane. Among the ions that can play a role, one of the most effective in screening is calcium [7]. The variation of extracellular free calcium leads to a different screening effect on the outer side of the membrane and this in turn leads to a change in the voltage drop across the membrane, that voltage dependent channels sense and respond to [8-10]

Vertebrate photoreceptors express a hyperpolarisation-activated current (*Ih*) responsible of the so called "sag" in the typical membrane potential response to flashes of light [11]. This current activates at membrane potentials below -60 mV, and has been found to be very sensitive to the aforementioned screening effect [12]. This makes it a good candidate to investigate the effect of different CSs at physiological concentrations on the gating properties of voltage-dependent ion channels recorded in physiological extracellular calcium concentration, which is the aim of the present work.

Material and Methods

Solutions

Since the effect observed in this work is very sensitive to extracellular ion concentrations, extreme care has been taken to assure that each solution used, especially control vs. CS-containing solutions, had the exact same pH, osmolality and chloride ions concentration. In fact, since chloride ions determine the junction potential between the Ag/AgCl electrode and the solution in the bath, unbalanced concentrations between control and test solutions give rise to a different junction potential that causes artefactual recordings.

All chemicals have been purchased from Sigma-Aldrich, Milan, Italy, unless otherwise specified. Concentrations are in mM.

Standard extracellular solution: NaCl, 110; KCl, 2.5; $CaCl_2$, 1; $MgCl_2$, 1.6; HEPES, 10; pH 7.6, final osmolality 242 mOsm/Kg adjusted with D-Glucose (usually less than 15 mM).

Intracellular solution: NaCl, 4; KCl, 52.7; K-Gluconate, 52.3; $MgCl_2$, 2.5; EGTA free acid 5; HEPES 10; pH 7.2; final osmolality 238 mOsm/Kg adjusted with D-Glucose (usually less than 10 mM).

CS solutions: chondroitin 4 sulfate (CS4) and chondroitin 6 sulfate (CS6) were purchased from Seikagaku (Tokyo, Japan) as di-sodium salts and were purified from whale and shark cartilage, respectively. The molecular mass of the CS4 and CS6 is about 20 and 43 kDa, respectively (Seikagaku, personal communication).We used a concentration of 15 mg/ml of CSs (see discussion), which corresponds to a concentration of 30 mM of CSs disaccharide. Given that the putative calcium binding site is composed by the disaccharide unit [13], this approach also helps to determine the concentration of the available calcium binding sites in the solution.

CS4 external solution: CS4-2Na, 30; NaCl, 50; KCl, 2.5; $CaCl_2$, 1; $MgCl_2$, 1.6; HEPES 10; pH 7.6; osmolality 242 mOsm/Kg adjusted with D-Glucose (usually less than 15 mM).

CS6 external solution: CS6-2Na, 30; NaCl, 50; KCl, 2.5; $CaCl_2$, 1; $MgCl_2$, 1.6; HEPES 10; pH 7.6; osmolality 242 mOsm/Kg adjusted with D-Glucose (usually less than 15 mM).

Extracellular control solution: Na-Gluconate, 60; NaCl, 50; KCl, 2.5; $CaCl_2$, 1; $MgCl_2$, 1.6; HEPES, 10; pH 7.6; osmolality 242 mOsm/Kg adjusted with D-Glucose (usually less than 15 mM).

For calcium current recording: extracellular: Tetra Ethyl Ammonium Chloride (TEA), 30; $CaCl_2$, 1; KCl, 2.5; $MgCl_2$, 1.6; HEPES, 10; CS4-2Na, 30; NaCl, 50; pH 7.6 with NaOH, osmolality 242 mOsm/Kg adjusted with D-Glucose (usually less than 7 mM).

Intracellular: N-methyl-D-glucamine, 95; TEA, 25; $MgCl_2$ 2.5; EGTA, 5; HEPES, 10; NaCl, 4; pH 7.2; osmolality 238 mOsm/Kg adjusted with D-Glucose (usually less than 5 mM).

CSs quantifications

To assess the purity of CSs used in this work, we used polyacrylamide gel electrophoresis of fluorophore-labeled saccharides (PAGEFS) technique [14]. Briefly, we prepared 1 mg/ml solution of CS4 and CS6, digested them with chondroitinase ABC (Sigma) and hyaluronidase SD (Seikagaku), derivatized the obtained unsaturated disaccharides with 2-aminoacridone (AMAC, Fluka) and separated them on polyacrylamide gels. To accurately measure the CS4 and CS6 disaccharides composition of *Xenopus laevis* retina, we dissected two retinas, removed proteins by proteinase K (Finnzymes) treatment and obtained the AMAC-labeled disaccharides as described above. Their quantification was performed by HPLC [14]. The water content of the retinas was obtained as $[(W_w-W_d)/W_w]*100$, where W_w is wet weight and W_d is dry weight.

Animal handling

Xenopus laevis have been housed in automated racks (XenoPlus, Tecniplast S.p.A., Buguggiate (VA) Italy) according to standard water parameters in 14/10 light/dark cycle. Animals were sacrificed according to the guidelines of the University of Insubria Ethical Committee. Eyeballs were removed and immediately processed for photoreceptor harvesting.

Photoreceptor dissociation procedure

In order to reduce the number of animals used in this work, one eyeball was kept in standard extracellular solution plus 2% foetal bovine serum (FBS) in an ice bath for the next day, while the other was immediately used for the experiment of the day. No differences in overall response have been observed between photoreceptors belonging to either eye. The eye was open by fine scissors along the *ora serrata* under stereomicroscopic view in a petri dish containing ice-cold extracellular solution plus 2% FBS. After removal of the cornea and lens, the retina was gently peeled off and divided into three small pieces. The three pieces were mechanically dissociated in a 0.5 ml volume of ice-cold extracellular solution plus 2% FBS in an eppendorf tube by means of gentle pipetting with a P1000 pipette. Fifty microliters of the photoreceptor suspension were plated onto 35mm petri dishes (Nunclon™ Δsurface, Nunc GmbH, Wiesbaden, Germany) on an ice bed and let settle for at least 30 minutes before adding 2 ml of extracellular control solution to the petri dish and begin the electrophysiological experiments.

Electrophysiological recording

The patch-clamp setup was composed of an inverted microscope (IM, Carl Zeiss, Heidelberg, Germany) equipped with an electromechanical manipulator (PatchMan, Eppendorf, Milan, Italy) for electrode fine/coarse movement, a mechanical manipulator (Narishige, Tokyo, Japan) to manually drive the fast multi-line solution changing head, an Axopatch 200B patch-clamp amplifier, a Digidata 1200B A/D board (Axon Instruments, now Molecular Devices, Sunnyvale, CA, USA), and a PC running Pclamp 6 software (Molecular Devices, Sunnyvale, CA, USA) for cell stimulation and data acquisition and analysis. Electrical zeroing of the pipette offset was performed in extracellular control solution, and a single cell was used in each petri dish to avoid contamination from previous experiments. Solutions were quickly changed onto the recorded cell by means of a manually operated multi-line perfusion head aligned with the cell. Solutions were gravity fed to the cells with a flow rate of 0.5 ml/min. Signals were filtered by the integrated low pass Bessel filter of the Axopatch 200B at 2 KHz and acquired at 10 KHz, stored on the PC and analysed off-line. Patch pipettes were pulled with a PP83 vertical puller (Narishige) from borosilicate glass capillaries (PG120T-7.5, Harvard Apparatus, Holliston, Massachusetts, USA). When filled with intracellular solution, their resistance in the bath was between 5.5- 6 MΩ. Access resistance was always < 10 MΩ and input resistance typically > 1.5 GΩ in all the cells considered for this work. Series resistance was compensated at 70% to avoid oscillation of the compensating circuit upon cell perfusion. Electrophysiological recordings have been obtained from light-adapted *Xenopus laevis* principal rods in the whole-cell configuration of the patch-clamp technique. Stimulation protocols are shown in the figures or described in the text where appropriate.

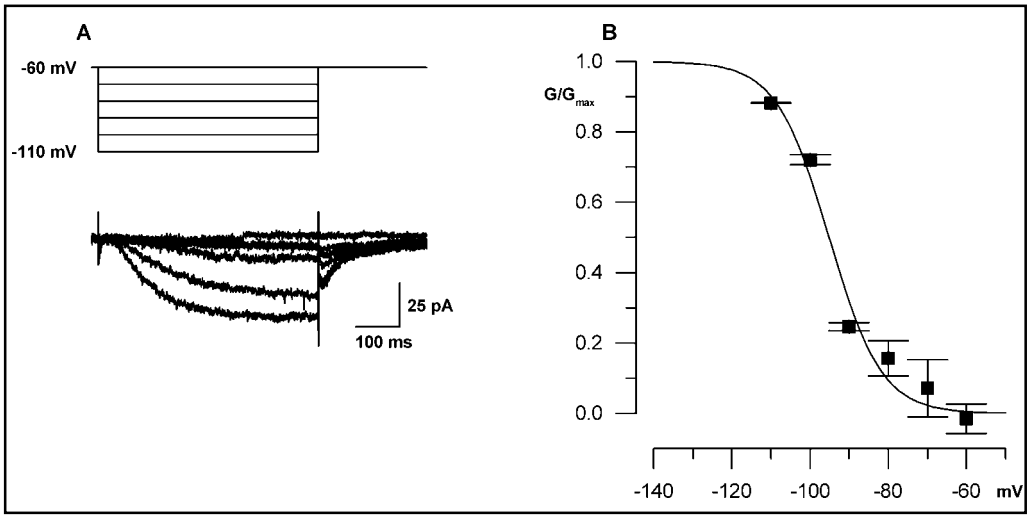

Fig. 1. (A). Current traces of *Ih* elicited in control external solution by means of the stimulation protocol showed in the upper panel. (B). Conductance-Voltage relationship of *Ih* obtained at steady-state by averaging the last 20 ms of each trace recorded at different membrane potentials like the ones reported in A, and superimposed Boltzman fitting (parameters given in the text).

Data fitting

Experimental data were fitted with the Boltzman equation in the form

$$G(V) = \frac{G_{max}}{1 + e^{\frac{V_{1/2} - V_m}{k}}}$$

with Origin software (Origin Lab, Northampton, MA, USA) where: G_{max} = maximum relative conductance with respect to control, $V_{1/2}$ = half-activation potential [mV], V_m = membrane potential [mV], k = slope factor [mV].

Atomic absorbance spectrometry

In order to obtain the chelation curve for CS4, 15 mg/ml solutions of CS4 in PBS buffer (Euroclone, without calcium) were prepared, containing 0, 1, 5, 10, 50, 100, and 200 mM of $CaCl_2$. To determine calcium bound to CS4, free calcium ions were separated from CS4 by gel filtration using PD10 column (GE healthcare) and eluted with PBS following a modification of the manufacturer's instruction. Briefly, the column was equilibrated with 25 ml of PBS without calcium, 2.5 ml of CS4 solution were loaded on the top of the column and the 2.5 ml of eluate were discarded. To elute CS4, 2.0 ml of PBS were loaded on the top of the column and the 2.0 ml of eluate were collected. Calcium bound to CS4 was quantified by using flame (air-acetylene) atomic absorbance spectrometry (AAS) on a Unicam Solaar M instrument equipped with a deuterium lamp. Wavelength (422.7 nm), band pass (0.5 nm), and all other instrumental parameters were set according to the usual recommendations of the instrument manufacturer. Moreover, lanthanum was added to the solutions to reduce interferences with matrix, after the methods in [15].

In order to compare the binding capability of various GAGs, 15 mg/ml solutions of CS4, CS6 and hyaluronan in PBS with 1 mM of $CaCl_2$ were prepared, free calcium was separated from GAG chelated calcium by using PD10, and calcium bound to GAGs was assayed as described above.

Data are presented as mean ± s.e.m. Statistical significance has been assessed with Student's *t-test* at $p<0.05$.

Results

Principal rods of *Xenopus laevis* display *Ih* current when hyperpolarised from a holding membrane potential of -60 mV (Fig. 1A, extracellular control solution). We used the activation curve of *h* current (control condition, $V_{1/2}$= -95.15 ± 0.19 mV, k= 6.72 ± 1.08 mV n=5 Fig.1B) as the very sensitive probe to investigate the possible effect of CSs on membrane potential (and thus on voltage-gated ion channels). Before proceeding with electrophysiological experiments, the same CS solutions used with rods have been assessed for purity and calcium binding properties. As the commercial CS4 and CS6 were purified from biological sources, we assessed their purity by using PAGEFS analysis and found that the two GAG solutions contained essentially the corresponding disaccharide without contamination from hyaluronan or unsulfated CS (Fig. 2A) indicating that each CS solution used had a very high degree of purity. The calcium binding capability of CS4 is shown in Figure 2B and, at calcium concentrations higher than 50 mM, saturation occurred. Since sulfation position modifies the chelating

Fig. 2. (A). PAGEFS analysis of CS4 and CS6 purity. One mg/ml solutions of CS4 and CS6 were treated with chondroitinase ABC and hyaluronidase SD to obtain GAG unsaturated disaccharides, and labelled with AMAC. The fluorotagged disaccharides were separated by PAGEFS and bands were visualized under UV light. Standard lane contains pure unsaturated disaccharides of CS4 (ΔCS-4S), CS6 (ΔCS-6S), hyaluronan (ΔHA), and chondroitin 0 sulfate (ΔCS-0S). (B) Calcium binding capability of CS4 at increasing calcium concentrations. Fifteen mg/ml of CS4 were incubated with increasing calcium concentrations, free calcium was separated to calcium bound to CS4 by gel filtration using PD10 column and bound calcium quantified by AAS. (C). Calcium binding capabilities of different GAGs. Fifteen mg/ml of solutions containing CS4, CS6, hyaluronan (HA), or no GAG (CNT) were incubated with 1 mM calcium and the calcium bound to each GAG was quantified as described in B. nd not detectable.

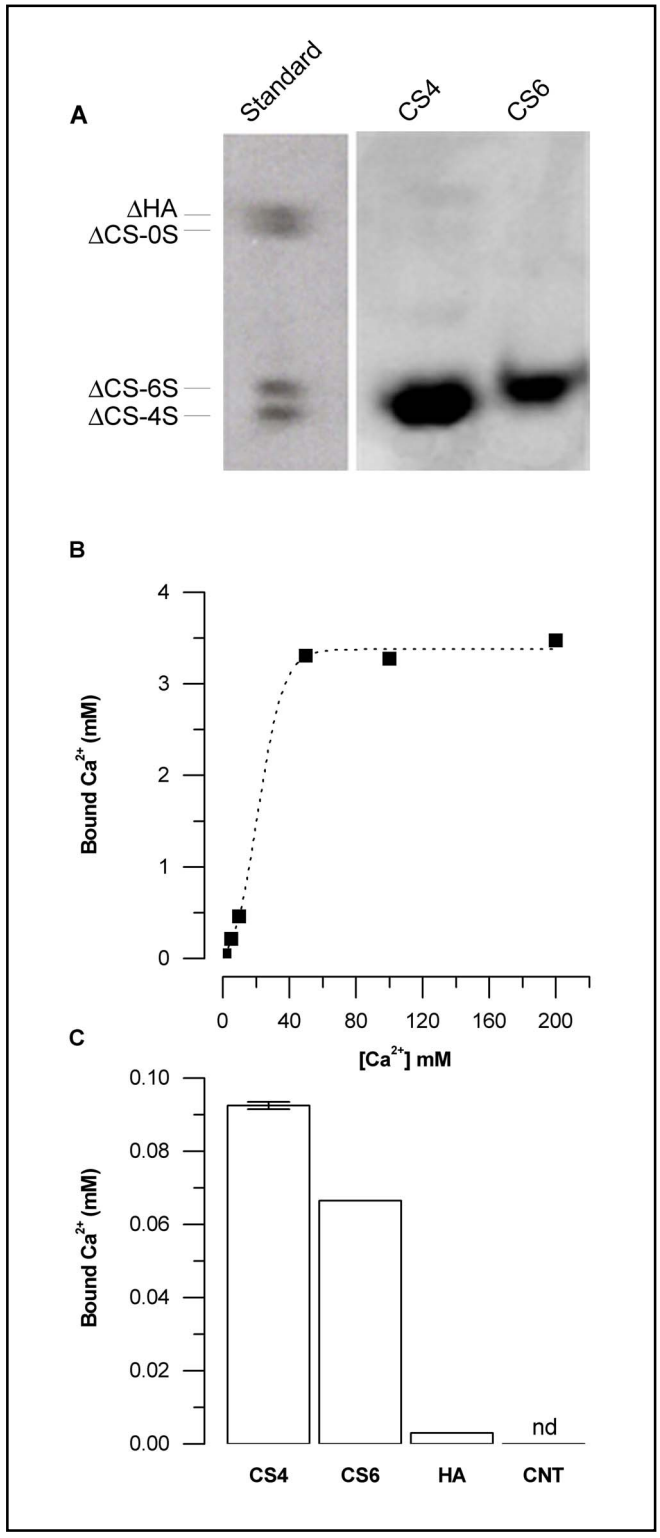

capabilities of CSs [16], we incubated the same amount of CS4 and CS6 with 1 mM calcium (Fig. 2C) and found that CS4 was able to bind significantly more calcium than CS6 (0.092 ± 0.001 mM for CS4 vs. 0.066 ± $4.03 \cdot 10^{-5}$ mM for CS6, $p<0.01$, n=3). The efficiency of the procedure to separate free calcium ions from those bound to CSs was verified by loading on the column a calcium solution without CSs and finding that, in the 2.0 ml of eluate, no calcium was detectable (Fig. 2C). Moreover, we loaded onto the PD10 column the calcium solution plus hyaluronan, another GAG known to have poor calcium chelating capabilities as it lacks sulfations [3], and found limited calcium associated with such GAG (Fig. 2C).

In CS4 solution, *Ih* activation curve significantly shifted to the left, and was fitted with a Boltzman equation with $V_{1/2}$ = -105.90 ± 0.65 mV ($\Delta V_{1/2}$ = -10.75 ± 1.24 mV, $p<0.01$ with respect to control, n=5), and k = 6.85 ± 0.68 mV (Fig. 3A, not significantly different from control).

When cells were superfused with CS6 containing solution, the *Ih* activation curve changed again with respect to control, but in a different way compared to CS4 perfusion (Fig 3B-C). In fact $V_{1/2}$ was significantly different from control (-102.17 ± 1.08 mV, $p<0.05$, n = 5), and not different from the $V_{1/2}$ obtained in CS4, but k did significantly change with respect to control (9.08 ± 1.12 mV, $p<0.05$, n=5). The superposition of the three fitted Boltzman equations obtained in the three conditions (Fig. 3D, control, solid line; CS4 perfusion, dashed line; CS6 perfusion, dotted line) shows a greater difference between CS4 and CS6 for voltage potentials near the activation threshold of *Ih*, whereas for lower membrane potentials close to the maximum activation of *Ih* the two plots are virtually identical. Moreover, while CS4 activation-shift effect encompasses all the activation range of *h* channels, CS6 curve is different from control curve only for midrange membrane potential values, as expected from the different slope factor *k*.

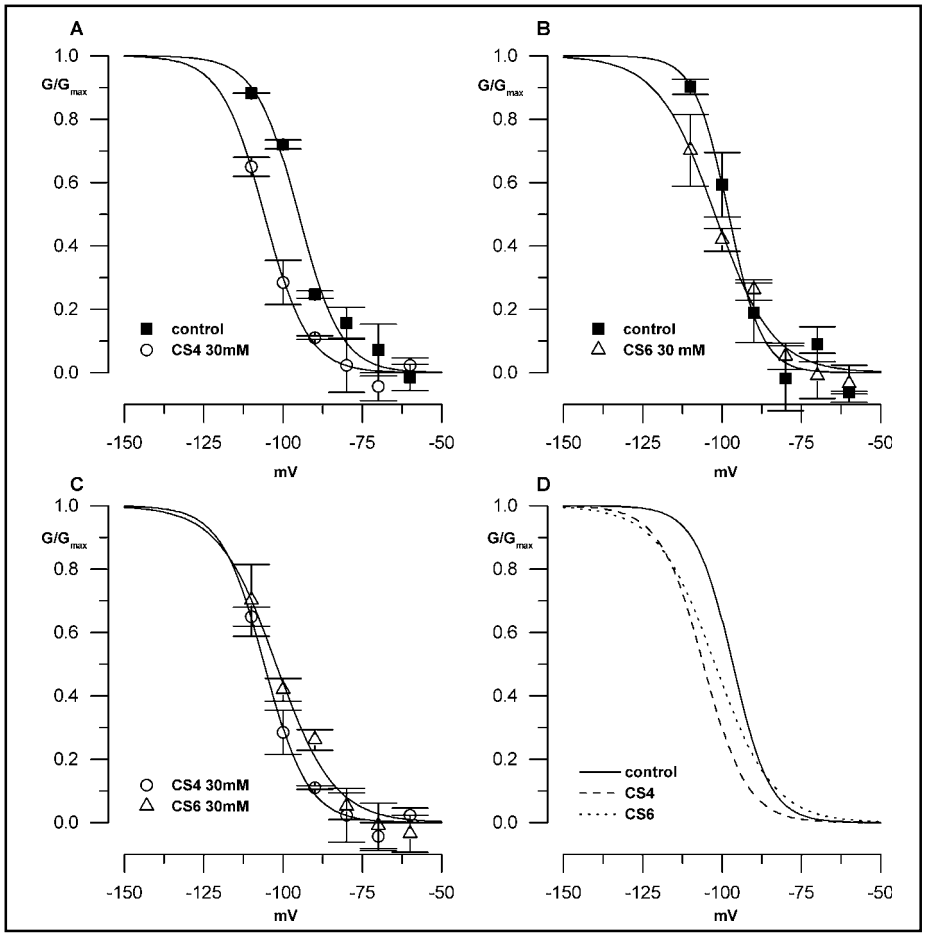

Fig. 3. G-V relationships and their respective superimposed Boltzman fits (parameters in the text): (A) in control (filled squares) or in the presence of CS4 (open circles). (B). in control (filled squares) or in the presence of CS6 (open triangles). (C). in CS4 perfused cells (open circles) and CS6 perfused cells (open triangles). (D). Boltzman fits in control (solid line), CS4 perfusion (dashed line) and CS6 perfusion (dotted line).

Since CS4 is known to be present in the plexiform layers of vertebrate retina [17, 18] we wanted to test the possibility that CS4 could alter the voltage-dependent calcium current present at the level of rod photoreceptors presynaptic terminals, which reside in the outer plexiform layer in intact retinas. The current-voltage (I-V) plots of actual calcium currents obtained both with voltage ramps and at steady state in 1mM extracellular calcium showed a leftward shift with respect to control both in steady-state I-V plot (Fig. 4A, wash trace omitted for clarity) and instantaneous I-V plots (Fig. 4B), with a shift of -10 mV of the peak current at steady-state. The time course of the calcium current (Fig. 4C) was not affected by the application of CS4. Effects of CS4 on calcium current were not readily reversed upon returning in control solution, as illustrated by the incomplete recovery of the current visible in figure 4C, *wash* trace. We next wanted to assess the effect on the voltage dependent calcium current of increasing concentrations of CS4. Figure 4D shows the averaged fitted Boltzman equations obtained from the activation curve of the voltage dependent calcium current recorded by voltage ramps as in figure 4B at different CS4 concentrations. Each Boltzman curve is the average of the single curves fitted on each of the 5 cells tested for each chondroitin solution. Table 1 summarises the values of $V_{1/2}$ and *k* in control (without CS4) and with increasing concentrations of CS4. It is worth to note that, while increasing the concentration of CS4 from 30 mM to 100 mM induces an additional leftward shift of -9.54 mV in $V_{1/2}$, decreasing CS4 concentration from 30 mM to 10 mM has a marginal effect on $V_{1/2}$. In fact, the effect on $V_{1/2}$ is almost statistically significant if compared to the control value also for a CS4 concentration of 10 mM. The slope factor *k* is never significantly different from control value or between different CS4 concentrations.

To further confirm that CS4 concentrations used in the electrophysiological experiments reflected the actual concentration of CS4 in *Xenopus laevis* retinas, we quantified the CSs by HPLC analysis of retinal extracted CSs. We found a retinal water content of 93%, in good agreement with the 84% found in rat retinas [19], also considering that *Xenopus* are fresh-water animals. CS4 and CS6 content were 0.005 mg/mg dry tissue weight and 0.0057 mg/mg dry tissue weight, respectively. The estimation of the extracellular volume of mamma-

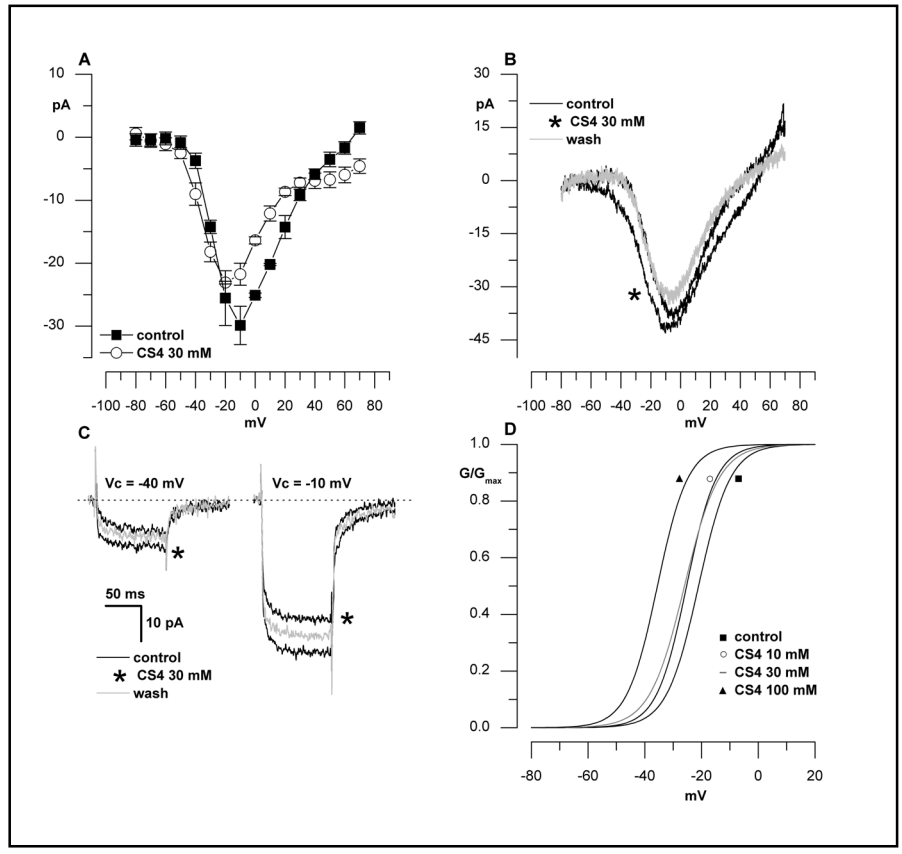

Fig. 4. (A). Steady-state current-voltage (I-V) plots of actual calcium current in isolated rods recorded in control condition (filled squares) and CS4 perfusion (open circles). *Wash* trace omitted for clarity. Data points are the average of the last 10 ms of the current traces elicited in response to a variable step stimulation protocol from -80 mV to + 80 mV in 10-mV increments of 100 msec of duration (as in C) (B). Istantaneous calcium current I-V plot of rods obtained with voltage ramps from -80 to +80 mV of 300 msec. duration. (C). Calcium current traces obtained at the specified membrane voltages from a holding potential of -60 mV. Asterisk, CS4 perfusion, *wash* trace in gray. (D) Dose effect of increasing CS4 concentrations on the activation curve of the voltage dependent calcium current of *Xenopus* rods. Each trace is the average Boltzman fit of single fits for each of the five cells used for each concentration. Grey trace corresponds to CS4 30 mM, which is the concentration used in the other experiments of panels A-C. Fit parameters are listed in table 1.

Table 1. *Student's t-test* values: * $p<0.05$ with respect to control; ** $p<0.05$ with respect to control, CS4 10 mM and CS4 30 mM; ° $p=0.057$ with respect to control. n=5 for all concentrations.

Dose effect of CS4 on $V_{1/2}$ and k for voltage dependent calcium current				
	Control	CS4 10 mM	CS4 30 mM	CS4 100 mM
$V_{1/2}$ (mV)	-21.06 ± 1.46	-25.27 ± 1.22°	-26.02 ± 1.06 *	-35.56 ± 2.91 **
k (mV)	5.62 ± 0.35	5.26 ± 0.46	6.26 ± 0.27	5.36 ± 0.69

lian retina has been elegantly and exhaustively performed in another work and found to be 1.80 ml/gr dry tissue weight [20]. Taken together, these data give average CS4 and CS6 concentrations in the whole retina of 2.78 and 3.16 mg/ml extracellular fluid, respectively, which are comparable to the concentrations we used in electrophysiological experiments (see Discussion for details).

Discussion

The calcium chelating properties of CSs have been studied in non physiological calcium solutions [3, 13]. Our present data show that even at physiological extracellular calcium concentration (1 mM), CS4 and CS6 display different calcium binding potencies due to their different sulfation position.

In ECM, CSs concentration ranges from 0 to 3 mg/g dry tissue weight [21]. However, since most of the tissue volume (especially in the central nervous system and highly packed tissues) is occupied by cells, the actual CSs concentration can be higher (up to ten times the measured one), as previously reported in the epidermis [22]. Hence, the CSs concentration used in the present work (15 mg/ml) may be a good estimate of the actual tissue concentration. In the retina, the chondroitin concentration obtained by us (see Results) can be regarded as a lower estimate of the actual concentration at the photoreceptor synapse, were the voltage-dependent calcium current is located. In fact, it is known that chondroitins accumulate in the so called

"Interphotoreceptor Matrix" (IPM) which surrounds rods and cones [18, 23, 24]. This causes a local increase of actual CSs quantity around photoreceptors compared to the average one we measured from the whole retina extracts, thus resulting in an uneven distribution of chondroitins in the whole retina. This in turn leads to an increase of the actual concentration at the photoreceptor synapse.

The leftward shift of the activation curve of *Ih* when cells were perfused with CS4 solution is compatible with what can be expected from the screening effect theory: the decrease of calcium concentration due to CS4 binding un-screens negative charges on the outer membrane surface, bringing the outer membrane potential closer to the value of the inner one, a phenomenon sensed as a "depolarisation" by the voltage sensors of voltage-dependent ion channels like the *h* channels. Thus, to obtain the same degree of activation with respect to control, the membrane potential had to be set to a more negative value.

Moreover, CS6 was able to shift the $V_{1/2}$ of *h* current activation to more negative potentials, but also modified the slope factor. This latter phenomenon has been seen in rod *h* current by increasing the extracellular pH [12]. However, this does not seem to be the case in the present work, since extracellular pH has always been carefully set to 7.6. However, it cannot be ruled out the possibility that the overall effect of CS6 on Ih could be the sum of the surface screening effect on$V_{1/2}$ and the activation of an intracellular pathway via a CS6 specific receptor which might alter the voltage sensitivity of the *h* channel. Specific CSs receptors are not known, but there is emerging evidence from the literature that CSs (the 2,4 di-sulfate form, at least) can act as co-factors, binding growth factors and activating one of the protein tyrosine phosphatase receptor PTP family [25]. HARE/Stabilin-1 is a hyaluronic acid scavenger receptor for endocitosis which is able to bind CS4 and CS6, too [26], so it cannot be completely excluded that the CS6-mediated effect on the slope factor might be due to the activation of a HARE- or PTP-like receptor.

In the functional assay on the photoreceptor calcium current, the I-V plots (Fig. 4) show the expected leftward-shift of the curve in CS4 challenged cells with respect to control. In principle one could also expect a diminution of the current peak, due to the decreased availability of free calcium at the outward channel pore. In our study this phenomenon has been observed in steady-state recordings only: in these experiments, before being stimulated with membrane test voltages in the range of the peak of calcium current (about -10 mV), cells have been perfused with CS4 for a longer period than cells stimulated with the ramp protocol. Hence, it could be inferred that the un-screening effect can be reached quickly, whereas the peak current reduction may need a more pronounced decrease in extracellular free calcium concentration attainable (at least in our conditions) by CS4 over a longer period of time.

The reduction in peak current observed in CS4 perfused cells (fig. 4C) is a real CS4-induced effect, not due to a "run-down" of calcium current itself: indeed, the current level in the *wash* (grey) trace obtained at -10mV is larger than the one obtained during CS4 perfusion. The lack of complete recovery could be ascribed to the fact that CSs tend to stick to the membrane, so that it is not possible to completely wash them away.

The dose effect of CS4 on the voltage activated calcium current of photoreceptors (Fig. 4D) shows that an increase of chondroitin sulfate in the extracellular matrix can proportionally induce a relevant leftward shift in the activation curve of voltage dependent ion channels, as expected from the Gouy-Chapman-Stern theory and the chelating properties of CS4. The almost statistically significant shift of $V_{1/2}$ obtained in CS4 10 mM solution (see Table 1 for values and statistical significance) could also indicate that even little amounts of chondroitin sulfate in the extracellular matrix might exert a significant effect on the gating properties of voltage dependent ion channels. Indeed, 10 mM chondroitin sulfate concentration equals to 5 mg/ml, a concentration very close to the one we measured as a lower estimate for the *Xenopus retina* and discussed above.

The impact of a leftward shift in the I-V curve of calcium current on the photoreceptor physiology is an augment of synaptic release of glutamate in the dark, which depends on the paradoxical increase of calcium entry through voltage-dependent calcium channels [27]. Since the normal dark resting potential of photoreceptors is set at about -40 mV, in the presence of CS4, calcium current is higher than control at -40 mV (Fig. 4A).

It is known that proteoglycans are present in the interphotoreceptor matrix surrounding rods and cones [18], and that horizontal cells express a specific type also at the level of ribbon synapses [28]. While there is general consensus that their presence in the IPM mediates significant interactions between photoreceptors and the retinal pigment epithelium, very little is known about their role in the synaptic process between photoreceptors and higher order cells. However, nyctalopin, a membrane-bound chondroitin sulphate proteoglygan, seems to be

involved in photoreceptor synapse proper functioning as well as in X-linked stationary night blindness [29-33]. It might therefore be possible that chondroitin composition of the photoreceptor ribbon synapse matrix could influence its function by way of the surface screening effect.

Neurite outgrowth is known to be affected by the chondroitin/hyaluronic acid composition of the ECM [34, 35], but at present there are supporting evidences that CSs may play a role by activating intracellular pathways rather than acting via a pure Gouy-Chapman-Stern mechanism [4, 36]. Given that the deposition of chondroitins in perineuronal nets seems to be activity-dependent [37], the results of the present work seem more consistent with a modulatory action of CSs on neural cells during normal function rather than during sprouting following injury or development.

However, a recent work on lamprey neurones [38] indicates that an increase in calcium current through L-type calcium channels results in an inhibition of neurite outgrowth. The same increase in calcium current is seen in a CS4 enriched environment, as our data suggest (Figure 4), and thus it is not possible to completely rule out the possibility that CSs could also act on axonal regeneration via a surface screening effect.

In conclusion, the present data indicate that CSs can bind calcium with different affinities, and this in turn can affect the transmembrane potential sensed by voltage gated ion channels. The effect of CS4 (and, to a lesser extent, of CS6) on neurones and other excitable cells would be a membrane depolarisation that could favour reaching of the threshold for spike generation. In fact neurones are surrounded by the so-called "perineuronal nets", composed of different PGs whose side chains are made mainly of CSs [39, 40]. It can be postulated that the GAGs composition of PGs might influence the electrical behaviour of excitable cells by way of the "surface screening" effect. Such a modulating role of the ECM GAGs with respect to the electrical behaviour of neurones might possibly explain why macromolecular ECM composition around many high-frequency spiking neurones is different from other areas of the nervous system [41-43], and / or why the decrease in CSs content in Alzheimer's disease correlates with the loss of function of parvalbumin-positive inhibitory interneurones [44].

Acknowledgements

A.M. wishes to thank Prof. Antonio Peres and Dott. Elena Bossi for hosting him in their laboratory, and Dott. Manuela Viola for precious discussions about CSs biochemistry. The authors are in debt with Prof. Alessandro Fumagalli, Giorgio Terzaghi and Raffaele Terzaghi for help with AAF. This work has been supported with FAR2006 from Università dell'Insubria to A.M.

References

1 Iozzo RV: Matrix proteoglycans: From molecular design to cellular function. Annu Rev Biochem 1998;67:609-652.

2 Handel TM, Johnson Z, Crown SE, Lau EK, Proudfoot AE: Regulation of protein function by glycosaminoglycans-as exemplified by chemokines. Annu Rev Biochem 2005;74:385-410.

3 Hunter GK, Wong KS, Kim JJ: Binding of calcium to glycosaminoglycans: An equilibrium dialysis study. Arch Biochem Biophys 1988;260:161-167.

4 Gilbert RJ, McKeon RJ, Darr A, Calabro A, Hascall VC, Bellamkonda RV: Cs-4,6 is differentially upregulated in glial scar and is a potent inhibitor of neurite extension. Mol Cell Neurosci 2005;29:545-558.

5 Hitchcock AM, Yates KE, Costello CE, Zaia J: Comparative glycomics of connective tissue glycosaminoglycans. Proteomics 2008;8:1384-1397.

6 Grahame DC: The electrical double layer and the theory of electrocapillarity. Chem Rev 1947;41:441-501.

7 Hille B, Woodhull AM, Shapiro BI: Negative surface charge near sodium channels of nerve: Divalent ions, monovalent ions and ph. Phil Trans R Soc Lond B 1975;270:301-318.

8 Hahin R, Campbell DT: Simple shifts in the voltage dependence of sodium channel gating caused by divalent cations. J Gen Physiol 1983;82:785-805.

9 Piccolino M, Byzov AL, Kurennyi DE, Pignatelli A, Sappia F, Wilkinson M, Barnes S: Low-calcium-induced enhancement of chemical synaptic transmission from photoreceptors to horizontal cells in the vertebrate retina. Proc Natl Acad Sci U S A 1996;93:2302-2306.

10 Piccolino M, Vellani V, Rakotobe LA, Pignatelli A, Barnes S, McNaughton P: Manipulation of synaptic sign and strength with divalent cations in the vertebrate retina: Pushing the limits of tonic, chemical neurotransmission. Eur J Neurosci 1999;11:4134-4138.

11 Bader CR, Bertrand D, Schwartz EA: Voltage-activated and calcium-activated currents studied in solitary rod inner segments from the salamander retina. J Physiol (Lond) 1982;331:253-284.

12 Malcolm AT, Kourennyi DE, Barnes S: Protons and calcium alter gating of the hyperpolarization-activated cation current (i(h)) in rod photoreceptors. Biochim Biophys Acta 2003;1609:183-192.

13 Grant D, Long WF, Moffat CF, Williamson FB: A study of ca(2+)-heparin complex-formation by polarimetry. Biochem J 1992;282 (Pt 2):601-604.

14 Karousou EG, Militsopoulou M, Porta G, De Luca G, Hascall VC, Passi A: Polyacrylamide gel electrophoresis of fluorophore-labeled hyaluronan and chondroitin sulfate disaccharides: Application to the analysis in cells and tissues. Electrophoresis 2004;25:2919-2925.
15 Crosa G, Stefani F, Bianchi C, Fumagalli A: Water security in uzbekistan: Implication of return waters on the amu darya water quality. Environ Sci Pollut Res Int 2006;13:37-42.
16 Tanaka K: Physicochemical properties of chondroitin sulfate. I. Ion binding and secondary structure. J Biochem 1978;83:647-653.
17 Souza AR, Kozlowski EO, Cerqueira VR, Castelo-Branco MT, Costa ML, Pavao MS: Chondroitin sulfate and keratan sulfate are the major glycosaminoglycans present in the adult zebrafish danio rerio (chordata-cyprinidae). Glycoconj J 2007;24:521-530.
18 Inatani M, Tanihara H: Proteoglycans in retina. Prog Retin Eye Res 2002;21:429-447.
19 Stefansson E, Wilson CA, Lightman SL, Kuwabara T, Palestine AG, Wagner HG: Quantitative measurements of retinal edema by specific gravity determinations. Invest Ophthalmol Vis Sci 1987;28:1281-1289.
20 Ames A, 3rd, Nesbett FB: Intracellular and extracellular compartments of mammalian central nervous tissue. J Physiol (Lond) 1966;184:215-238.
21 Calabro A, Midura RJ, Hascall VC, Plaas A, Goodstone NJ, Roden L: Structure and biosynthesis of chondroitin sulfate and hyaluronan; in Iozzo RV (ed) Proteoglycans: Structure, biology, and molecular interactions. New York, Marcel Dekker Inc., 2000, pp 5-26.
22 Tammi R, Tammi M: Hyaluronan in epidermis, 1998, In Glycoforum: Science of Hyaluronan today. URL:http://www.glycoforum.gr.jp/science/hyaluronan/HA04/HA04E.html
23 Tawara A, Varner HH, Hollyfield JG: Proteoglycans in the mouse interphotoreceptor matrix. I. Histochemical studies using cuprolinic blue. Exp Eye Res 1988;46:689-704.
24 Varner HH, Rayborn ME, Osterfeld AM, Hollyfield JG: Localization of proteoglycan within the extracellular matrix sheath of cone photoreceptors. Exp Eye Res 1987;44:633-642.
25 Sugahara K, Mikami T, Uyama T, Mizuguchi S, Nomura K, Kitagawa H: Recent advances in the structural biology of chondroitin sulfate and dermatan sulfate. Curr Opin Struct Biol 2003;13:612-620.
26 Harris EN, Weigel PH: The ligand-binding profile of hare: Hyaluronan and chondroitin sulfates a, c, and d bind to overlapping sites distinct from the sites for heparin, acetylated low-density lipoprotein, dermatan sulfate and cs-e. Glycobiology 2008
27 Cadetti L, Thoreson WB, Piccolino M: Pre- and post-synaptic effects of manipulating surface charge with divalent cations at the photoreceptor synapse. Neuroscience 2004;129:791-801.
28 Williams C, Villegas M, Atkinson R, Miller CA: Chondroitin sulfate proteoglycan specific to retinal horizontal neurons. J Comp Neurol 1998;390:268-277.
29 Bahadori R, Biehlmaier O, Zeitz C, Labhart T, Makhankov YV, Forster U, Gesemann M, Berger W, Neuhauss SC: Nyctalopin is essential for synaptic transmission in the cone dominated zebrafish retina. Eur J Neurosci 2006;24:1664-1674.
30 Bech-Hansen NT, Naylor MJ, Maybaum TA, Sparkes RL, Koop B, Birch DG, Bergen AA, Prinsen CF, Polomeno RC, Gal A, Drack AV, Musarella MA, Jacobson SG, Young RS, Weleber RG: Mutations in nyx, encoding the leucine-rich proteoglycan nyctalopin, cause x-linked complete congenital stationary night blindness. Nat Genet 2000;26:319-323.
31 Gregg RG, Kamermans M, Klooster J, Lukasiewicz PD, Peachey NS, Vessey KA, McCall MA: Nyctalopin expression in retinal bipolar cells restores visual function in a mouse model of complete x-linked congenital stationary night blindness. J Neurophysiol 2007;98:3023-3033.
32 Morgans CW, Ren G, Akileswaran L: Localization of nyctalopin in the mammalian retina. Eur J Neurosci 2006;23:1163-1171.
33 Pusch CM, Zeitz C, Brandau O, Pesch K, Achatz H, Feil S, Scharfe C, Maurer J, Jacobi FK, Pinckers A, Andreasson S, Hardcastle A, Wissinger B, Berger W, Meindl A: The complete form of x-linked congenital stationary night blindness is caused by mutations in a gene encoding a leucine-rich repeat protein. Nat Genet 2000;26:324-327.
34 Sherman LS, Back SA: A 'gag' reflex prevents repair of the damaged cns. Trends Neurosci 2008;31:44-52.
35 Busch SA, Silver J: The role of extracellular matrix in cns regeneration. Curr Opin Neurobiol 2007;17:120-127.
36 Gama CI, Tully SE, Sotogaku N, Clark PM, Rawat M, Vaidehi N, Goddard WA, 3rd, Nishi A, Hsieh-Wilson LC: Sulfation patterns of glycosaminoglycans encode molecular recognition and activity. Nat Chem Biol 2006;2:467-473.
37 Dityatev A, Bruckner G, Dityateva G, Grosche J, Kleene R, Schachner M: Activity-dependent formation and functions of chondroitin sulfate-rich extracellular matrix of perineuronal nets. Dev Neurobiol 2007;67:570-588.
38 McClellan AD, Kovalenko MO, Benes JA, Schulz DJ: Spinal cord injury induces changes in electrophysiological properties and ion channel expression of reticulospinal neurons in larval lamprey. J Neurosci 2008;28:650-659.
39 Carulli D, Rhodes KE, Brown DJ, Bonnert TP, Pollack SJ, Oliver K, Strata P, Fawcett JW: Composition of perineuronal nets in the adult rat cerebellum and the cellular origin of their components. J Comp Neurol 2006;494:559-577.
40 Celio MR, Spreafico R, De Biasi S, Vitellaro-Zuccarello L: Perineuronal nets: Past and present. Trends Neurosci 1998;21:510-515.
41 Vitellaro-Zuccarello L, Bosisio P, Mazzetti S, Monti C, De Biasi S: Differential expression of several molecules of the extracellular matrix in functionally and developmentally distinct regions of rat spinal cord. Cell Tissue Res 2007;327:433-447.
42 Hartig W, Singer A, Grosche J, Brauer K, Ottersen OP, Bruckner G: Perineuronal nets in the rat medial nucleus of the trapezoid body surround neurons immunoreactive for various amino acids, calcium-binding proteins and the potassium channel subunit kv3.1b. Brain Res 2001;899:123-133.
43 Morris NP, Henderson Z: Perineuronal nets ensheath fast spiking, parvalbumin-immunoreactive neurons in the medial septum/diagonal band complex. Eur J Neurosci 2000;12:828-838.
44 Baig S, Wilcock GK, Love S: Loss of perineuronal net n-acetylgalactosamine in alzheimer's disease. Acta Neuropathol 2005;110:393-401.